

Frequency Response Analysis of Diaphragm for Small Earphone

Supported by Nonlinear Springs with Hysteresis Using Finite Element Method

Manabu SASAJIMA*, Takao YAMAGUCHI**, Yoshio KOIKE*, Akira HARA*,

Ken-ichi NAGAI**, Shinichi MARUYAMA**

*Foster Electric Co., Ltd., 512 Miyazawa-cho, Akishima, Tokyo, Japan, sasajima@foster.co.jp

**Gunma University, tenjin-cho 1-5-1, Kiryu, Gunma, Japan

Abstract

To check and remove distortion of sound reproduction in high-specs small earphones, it is of importance to evaluate and clarify nonlinearity in vibrations of elastic diaphragms in the earphones. This paper describes vibration analysis using three-dimensional finite element method for elastic diaphragm supported by multiple nonlinear concentrated springs with linear hysteresis damping. The restoring forces of the springs have cubic nonlinearity. Finite element for the nonlinear springs with hysteresis are expressed and are connected to the elastic diaphragm modeled by linear solid finite elements in consideration of complex modulus of elasticity. Further, the discretized equations in physical coordinate are transformed into the nonlinear ordinary coupled equations using normal coordinate corresponding to linear natural modes. Moreover, by using Modal Strain Energy Method, modal loss factors are approximately computed from complex eigenvalue problem and are introduced into the nonlinear ordinary coupled differential equations. This transformation yields computation efficiency. In this study, the shape of the elastic diaphragm for the small earphone is cone. The cone is supported by the nonlinear springs with hysteresis on the all edges. By carrying out eigenvalue analysis, we calculated resonant frequencies and eigenmodes. Using these modal parameters, resonance responses are computed under various amplitudes of excitation. The calculated resonance responses by the proposed method were verified by experimental responses. In the vicinity of the uniform translation mode in out-of-plane direction of the cone, the calculated and the experimental resonance responses show the characteristics of hardening type. Moreover, third super harmonic resonance responses of this mode appeared both in the calculation and the experiment.

Key words: Electric Equipment, Damping, Nonlinear Vibration, Finite Element Method

1. Introduction

In a typical speaker, the diaphragm has a soft part called the “edge” on its peripheral portion. The purpose of the edge is to move the diaphragm in the out of plane direction by deforming significantly. However, vibration of the diaphragms often used in small earphones, tends to deform the whole diaphragm. This is because the diaphragm in this type of speaker has no equivalent to the edge part. The stiffness of this diaphragm type can be controlled by design variables, such as the size and shape of the outer diameter. For example, a dome shape, a spiral, or concentric grooves (called corrugation) can be used, but predicting their frequency characteristics is difficult. Because the diaphragm is very thin and geometrically complex, there are often differences between the design shape and the actual shape. When designing the shape of the diaphragm, it is common to create a three-dimensional model and make predictions of the frequency characteristics of small amplitude analysis using the finite element method (FEM). However, for high input conditions, the relationship between load and displacement of the diaphragm is expected to be nonlinear. Due to the recent trend of further miniaturization of the driver unit (including the diaphragm), it has become necessary to increase the relative amplitude for a given diaphragm size, in order to obtain the required output. As a result, the nonlinear distortion of the sound has tended to increase. Many researchers have examined the nonlinear vibration problem of a diaphragm in the lumped approximation. For example, Yoshihisa investigated nonlinear distortion and the jumping phenomenon when the diaphragm amplitude is large⁽¹⁾, and Imaoka et al. proposed the dynamic strain measurement method as a way of evaluating the nonlinearity of the sound of a small speaker⁽²⁾. Sato et al. focused on the nonlinearity of the speaker diaphragm, when treated as a lumped stiffness, as a cause of harmonic distortion and the occurrence

of jumping phenomenon⁽³⁾⁽⁴⁾. They considered the measurement method and performed an analysis using the equivalent circuit. However, a nonlinear analysis treating the diaphragm as a continuous body has not been made. Meanwhile, as a method of nonlinear analysis, Kondo et al. proposed a high-speed stability criterion for the study of the vibration characteristics of nonlinear systems containing concentrated springs⁽⁵⁾. This was applied to the forced vibration of the structure and supported by a nonlinear-coupled beam. Shaw et al. proposed a nonlinear modal analysis, and applied this to a simply supported beam attached to a nonlinear concentrated spring at the midpoint of the beam⁽⁶⁾. Yamaguchi et al. proposed a fast numerical method to compute the nonlinear vibrations of systems involving elastic blocks and a nonlinear concentrated spring^{(7),(8)}. In the analysis of Yamaguchi et al., a fast-response computation method is developed by introducing normal coordinates corresponding to the linear natural modes. They extended this method, by formulating a calculation of the response of a viscoelastic block that is attached to a nonlinear concentration spring, where the restoring force is given as a linear hysteretic damping⁽⁹⁾. In this paper, the analyses mentioned above are applied⁽⁵⁾⁻⁽⁸⁾. First, the property of a nonlinear spring is identified by measuring the relationship between load and displacement of the diaphragm. Then, the resonant response is analyzed, using FEM as an elastic diaphragm supported by multiple concentrated nonlinear springs with hysteresis. In particular, all nodes on the periphery of the elastic diaphragm are supported by multiple nonlinear springs with hysteresis acting in an out of plane direction. The elastic plate is supported by linear concentrated springs acting in an in-plane direction. We also analyze the dynamic response of periodic excitation forces applied in an out of plane direction. The discrete nonlinear equations are transformed into motion equations with respect to the coordinates of the natural vibration modes. We then apply these equations to a large degree of freedom problem. To speed up the analysis, we reduce the degrees of freedom of the diaphragm response, such that nonlinearity only occurs in the reaction force of the concentrated nonlinear springs, and not in the diaphragm geometry. To verify the proposed method of analysis, a comparison study is performed by measuring the displacement response and response of the diaphragm of the earphone using a laser displacement meter.

2. Simulation model

Figure 1 shows the simulation model. The shape of the diaphragm near the center of the cone, and the electrical conductor which vibrates together with the diaphragm, are modeled by finite elements. When we made this FE model, we used HyperMesh v10.0 (Altair Engineering Inc.) at meshing. The model is 7 [mm] in diameter and 10 [μ m] thick. And the cone of the diaphragm is 1.0 [mm] in height. The density of the diaphragm cone and the electrical conductor are 6.12×10^2 [kg/m³] and 8.78×10^3 [kg/m³], respectively. We introduce stiffness elements behind the diaphragm in consideration of the complaisance of air in this region. The origin of the model coordinates is at the center bottom of the xy-plane of the diaphragm, and the vibration is in the z-direction. The reference point of the z-direction displacement is near the center of the diaphragm. Assuming the deformations are small, the elastic diaphragm and electrical conductor are modeled by an eight-node isoparametric solid element model, in consideration of the non-conforming mode for FEM⁽¹⁰⁾⁻⁽¹¹⁾. Concentrated springs are connected to the peripheral of the diaphragm cone, in the x-, y-, and z-directions, only the z-direction springs are nonlinear. Fig. 2 shows the relation between restoring force R_{mz} and displacement U_{mz} of the nonlinear static spring. In this dynamic analysis, the nonlinear springs have hardening type of restoring force and are subject to hysteresis.

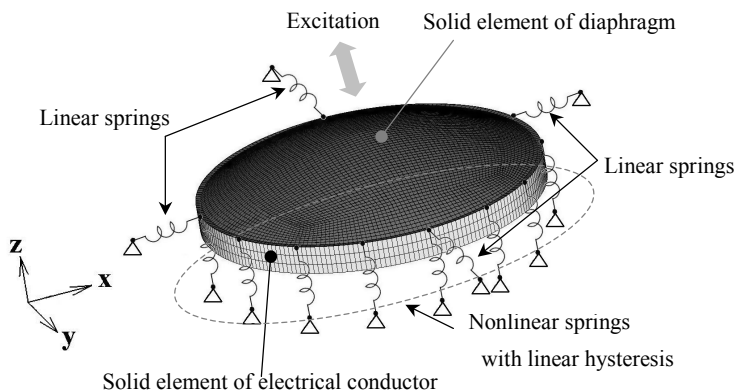


Fig. 1 Simulation model

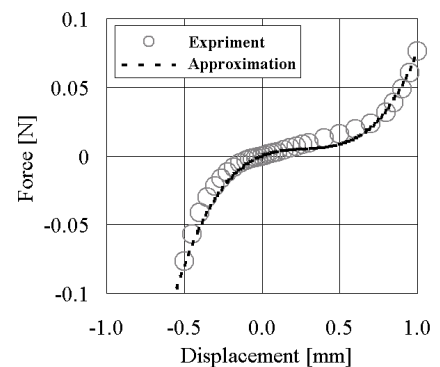


Fig. 2 Restoring force of nonlinear concentrated springs

3. Numerical method

As shown in Fig. 1, we consider the case that the elastic cone of the diaphragm and the electrical conductor are supported by nonlinear springs around the edge. We now discretized the equations obtained by modeling the system with finite elements.

3.1 Discretized equation of nonlinear springs

The restoring force of the springs is expressed as $R_{mz} = \gamma_{1mz} U_{mz} + \gamma_{2mz} U_{mz}^2 + \gamma_{3mz} U_{mz}^3$ ($m=1, 2, 3, \dots$). We denote displacement in the z-direction at the nodal point α_m as U_{mz} , where the nonlinear concentrated spring with a diaphragm. These relations can be rewritten in matrix form as

$$\begin{aligned} \{R_m\} &= [\bar{\gamma}_{1m}] \{U_s\} + \{\bar{d}_m\} \\ \{R_m\} &= \{\gamma_{mx}, \gamma_{my}, \gamma_{mz}\}^T, \quad \{U_s\} = \{U_{mx}, U_{my}, U_{mz}\}^T, \\ \{\bar{d}_m\} &= \{0, 0, \gamma_{2mz} U_{mz}^2 + \gamma_{3mz} U_{mz}^3\}^T \end{aligned} \quad (1)$$

where $R_{mx} = R_{my} = 0$. In Eq. (1) $\{R_m\}$ is a vector containing nonlinear terms of the restoring force of m, $\{U_s\}$ is the nodal displacement vector, $[\bar{\gamma}_{1m}]$ is the linear stiffness matrix, and $\{\bar{d}_m\}$ contain the nonlinear terms of the restoring force. Further, linear hysteresis damping is introduced as $\gamma_{1mz} = \bar{\gamma}_{1mz} (1 + j\eta_s)$, where $\bar{\gamma}_{1mz}$ is the real part of γ_{1mz} , and η_s is the material loss factor of the concentrated spring. j is the imaginary unit.

3.2 Discretized equation of the elastic cone of the diaphragm

Under the assumption of small oscillations, the diaphragm cone can be modeled by three-dimensional linear finite elements. The particle displacement vector $\{U_d\}$ in the region of an element is set as $\{U_d\} = \{U_x, U_y, U_z\}^T$. The relation between the particle displacement vectors $\{U_d\}$ and $\{U_e\}$, both at nodal points in the element, can then be approximated as follows:

$$\{U_d\} = [N]^T \{U_e\} \quad (2)$$

where $[N]^T$ represents a matrix comprised of the appropriate shape function. Vectors of stress $\{\sigma\} = \{\sigma_x, \sigma_y, \sigma_z, \tau_{xy}, \tau_{yz}, \tau_{zx}\}^T$ and strain $\{\varepsilon\} = \{\varepsilon_x, \varepsilon_y, \varepsilon_z, \gamma_{xy}, \gamma_{yz}, \gamma_{zx}\}^T$ are related as below:

$$\{\sigma\} = [D] \{\varepsilon\} \quad (3)$$

where $[D]$ is the matrix of elastic modulus E_e and Poisson's ratio ν_e . Strain energy, kinetic energy, and external work are obtained from Eq. (2), (3). The following expression can be derived by applying the principle of virtual work for an elastic diaphragm without spring elements.

$$[M_f] \{\ddot{U}_f\} = -[K_f] \{U_f\} + \{F_f\} \quad (4)$$

where $[M_f]$, $[K_f]$, $\{U_f\}$ and $\{F_f\}$ are mass matrix, complex stiffness matrix, displacement vector, and nodal force vector, respectively, and $\dot{\cdot}$ denotes the time derivative. Further the complex stiffness matrix of the behind air layer is added.

3.3 Discrete equations for the combined system of the diaphragm cone and the nonlinear concentrated springs

The restoring force $\{R_m\}$ is added to the nodal force at the attached node α_m between concentrated springs and the diaphragm. The following expression for the global system can then be obtained:

$$\begin{aligned} [M]\{\ddot{U}\} &= -[K]\{U\} - \{\hat{d}\} + \{F\} \\ \{\hat{d}\} &= \sum_m \{\hat{d}_m\} \end{aligned} \quad (5)$$

where $[M]$, $[K]$, $\{U\}$, $\{F\}$ are the mass matrix, complex stiffness matrix, displacement vector, and external force vector in the global system, respectively. $\{\hat{d}_m\}$ is modified from $\{\bar{d}_m\}$ so as to have an identical vector size to the number of degree of freedom(dof) of the global system.

3.4 Approximate expression for modal damping

By neglecting both the nonlinear term and the external force vector in Eq. (5), and by assuming $\{U\} = \{\phi\}e^{j\omega t}$ (t : time), we can obtain the following eigenvalue problem:

$$\sum_{e=1}^{e_{\max}} ([K_R]_e (1 + j\eta_e) - (\omega^{(i)})^2 (1 + j\eta_{tot}^{(i)}) [M]_e) \{\phi^{(i)}\} = \{0\} \quad (6)$$

In this equation, superscript (i) stands for the i -th eigenmodes, $(\omega^{(i)})^2$ is the real part of the complex eigenvalue, $\{\phi^{(i)}\}$ is the complex eigenvector, and $\eta_{tot}^{(i)}$ is the modal loss factor. Next, we introduce the material loss factor for each element, η_e ($e=1, 2, 3, \dots, e_{\max}$), and define β_e as

$$\beta_e = \eta_e / \eta_{\max}, \beta_e \leq 1 \quad (7)$$

Assuming that the maximum loss factor $\eta_{\max} \ll 1$, solutions of Eq. (6) are expanded using the small parameter $\mu = j\eta_{\max}$:

$$\{\phi^{(i)}\} = \{\phi^{(i)}\}_0 + \mu\{\phi^{(i)}\}_1 + \mu^2\{\phi^{(i)}\}_2 + \dots \quad (8)$$

$$(\omega^{(i)})^2 = (\omega_0^{(i)})^2 + \mu^2(\omega_2^{(i)})^2 + \mu^4(\omega_4^{(i)})^2 + \dots \quad (9)$$

$$j\eta_{tot}^{(i)} = \mu\eta_1^{(i)} + \mu^3\eta_3^{(i)} + \mu^5\eta_5^{(i)} + \mu^7\eta_7^{(i)} + \dots \quad (10)$$

In these equations, under conditions of $\beta_e \leq 1$ and $\eta_{\max} \ll 1$, we have that $\beta_e\eta_{\max} \ll 1$. Thus, $\mu\beta_e$ is regarded as a small parameter, of the order of μ . In the above equations, $\{\phi^{(i)}\}_0$, $\{\phi^{(i)}\}_1$, \dots , $(\omega_0^{(i)})^2$, $(\omega_2^{(i)})^2$, \dots and $\eta_1^{(i)}$, $\eta_3^{(i)}$, \dots have real quantities. Substituting Eq. (8)-(10) into Eq. (6), the following equation can be derived:

$$\eta_{tot}^{(i)} = \sum_{e=1}^{e_{\max}} (\eta_e S_e^{(i)}), \quad S_e^{(i)} = \{\phi^{(i)}\}_0^T [K_R]_e \{\phi^{(i)}\}_0 / \sum_{e=1}^{e_{\max}} (\{\phi^{(i)}\}_0^T [K_R]_e \{\phi^{(i)}\}_0) \quad (11)$$

where $S_e^{(i)}$ is each elements' share of the total strain energy. The eigenmodes $\{\phi^{(i)}\}_0$ in Eq. (8) are real. According to these expressions, the mode loss factor $\eta_{tot}^{(i)}$ can be calculated using the material loss factors η_e and share of the total strain energy $S_e^{(i)}$ of each element. $\eta_e S_e^{(i)}$ is equal to the amount of energy dissipated in the division of each element.

3.5 Conversion from the discretized equations in physical coordinates to the nonlinear equation in normal coordinates

It takes a large amount of computational time to directly calculate Eq. (5) in physical coordinates. In this section, a numerical manipulation is proposed to decrease the number of dof for the discretized equations of motion. First, we assume that the linear natural modes $\{\phi^{(i)}\}$ of vibration can be approximated to $\{\phi^{(i)}\}_0$. Next, by introducing normal coordinates \tilde{b}_i corresponding to the linear natural modes $\{\phi^{(i)}\}_0$, the modal displacement vector $\{U\}$ can be expressed using both $\{\phi^{(i)}\}_0$ and \tilde{b}_i as follows:

$$\begin{aligned} \{U\} &= \sum_{i=1} (1/n_i) \tilde{b}_i \{\tilde{\phi}^{(i)}\}_0 \quad (12) \\ \{\phi^{(i)}\}_0 &= \{\tilde{\phi}^{(i)}\}_0 / n_i, \quad m_i = \{\phi^{(i)}\}_0^T [M] \{\phi^{(i)}\}_0, \quad n_i = (m_i)^{-(1/2)}, \\ \{\tilde{\phi}^{(i)}\}_0^T [M] \{\tilde{\phi}^{(i)}\}_0 &= 1 \end{aligned}$$

By substituting Eq. (12) into Eq. (5), the following nonlinear ordinary simultaneous equations in the normal coordinates \tilde{b}_i can be obtained as

$$\begin{aligned} M(\tilde{b}_i) &\equiv \ddot{\tilde{b}}_i + \eta_{tot}^{(i)} \omega_0^{(i)} \dot{\tilde{b}}_i + (\omega_0^{(i)})^2 \tilde{b}_i \quad (13) \\ &+ \sum_j \sum_k \tilde{D}_{ijk} \tilde{b}_j \tilde{b}_k + \sum_j \sum_k \sum_l \tilde{E}_{ijkl} \tilde{b}_j \tilde{b}_k \tilde{b}_l - \tilde{P}_i = 0 \quad (i, j, k, l = 1, 2, 3, \dots) \\ \tilde{P}_i &= n_i \{\tilde{\phi}^{(i)}\}_0^T \{F\}, \quad \tilde{D}_{ijk} = \sum_{m=1} \gamma_{2mz} (n_i / (n_j n_k)) \tilde{\phi}_{cmzi} \tilde{\phi}_{cmzj} \tilde{\phi}_{cmzk} \\ \tilde{E}_{ijkl} &= \sum_{m=1} \gamma_{3mz} (n_i / (n_j n_k n_l)) \tilde{\phi}_{cmzi} \tilde{\phi}_{cmzj} \tilde{\phi}_{cmzk} \tilde{\phi}_{cmzl}, \quad \{\tilde{\phi}^{(i)}\}_0 = \{\tilde{\phi}_{1Xi}, \tilde{\phi}_{1Yi}, \tilde{\phi}_{1zi}, \tilde{\phi}_{2Xi}, \tilde{\phi}_{2Yi}, \tilde{\phi}_{2zi}, \tilde{\phi}_{3Xi}, \dots\}^T \end{aligned}$$

$\tilde{\phi}_{cmzi}$ is the z-direction component of displacement $\{\tilde{\phi}^{(i)}\}_0$ at connecting points α_m of the nonlinear springs and the elastic diaphragm. As Eq. (13) has fewer dof than Eq. (5), we can save a significant amount of computational time.

3.6 Nonlinear periodic response

We consider the external force \tilde{P}_i to be a periodic excitation, as $\tilde{P}_i = P_{di} \cos \omega t$ (ω : excitation frequency). To determine the periodic response, the response to this periodic excitation is given by considering super harmonic components $2\omega, 3\omega, \dots$, subharmonic components $(1/2)\omega, (1/3)\omega, \dots$, and ultra-subharmonic components $(3/2)\omega, (2/3)\omega, \dots$, of the excitation frequency.

$$\begin{aligned} \tilde{b}_i &= C_{i1\kappa 0} + \sum_p [C_{i1\kappa p} \cos(\kappa p \omega t) + C_{i2\kappa p} \sin(\kappa p \omega t)] \quad (14) \\ (i &= 1, 2, 3, \dots, p = 1, 2, 3, \dots, \kappa = 1, 1/2, 1/3, \dots) \end{aligned}$$

where $C_{i1\kappa p}$, $C_{i2\kappa p}$ are undetermined coefficients. To determine the principal resonance and super harmonic resonance response, the value $\kappa=1$ is used. To determine the subharmonic resonance response, $\kappa=1/n$ (n : integer) is used. By substituting Eq. (14) into Eq. (13) and applying the harmonic balance method, we obtain

$$\begin{aligned} ((\kappa s \omega) / 2\pi) \int_0^{2\pi / (\kappa s \omega)} M(\tilde{b}_i) \sin(\kappa s \omega t) dt &= 0 \quad (s = 1, 2, \dots) \quad (15) \\ ((\kappa s \omega) / 2\pi) \int_0^{2\pi / (\kappa s \omega)} M(\tilde{b}_i) \cos(\kappa s \omega t) dt &= 0 \quad (s = 0, 1, 2, \dots) \end{aligned}$$

In solving the simultaneous cubic equations from the above formulae for C_{i1kp}, C_{i2kp} , the periodic solution of the resonant response is obtained using the Newton-Raphson method. At reference points ξ , the z-component W_{rms} of the amplitude root mean square(rms) value of the response is calculated.

4. Verification of calculation

We measured the vibration displacement response near the center of an earphone with a laser displacement meter, for comparison with our calculation results.

4.1 Measurement system

Figure 3 shows the system of measurement. The signal made by the function generator is amplified by the headphone amplifier. The signal is then output to the earphone. The output signal is a sine wave that is sweeping from 20 [Hz] to 20,000 [Hz]. The displacement of the diaphragm is measured by a laser displacement meter. The spot diameter of the laser displacement meter is $25 [\mu m] \times 1400 [\mu m]$. The sampling period is 10 [μs].

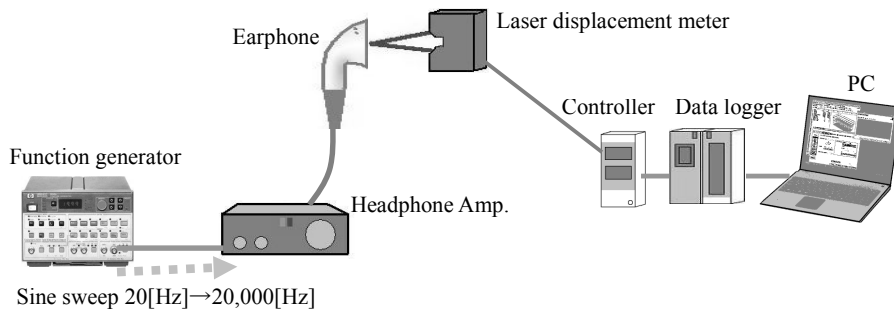


Fig. 3 System of Measurement

4.2 Frequency response

Figure 4 shows calculated eigenmodes and each resonant frequency. We compared the response analysis and the measurements from the laser displacement meter. The diaphragm had a Young's modulus of 3.07 [GPa] and a Poisson's ratio of 0.29. The Young's modulus of the electrical conductor is 33.0 [GPa]. Coefficients for the restoring force of the concentrated springs are set as $\bar{\gamma}_{1mz} = 4.54 \times 10^{-3} [N/mm]$, $\gamma_{2mz} = 1.53 \times 10^{-2} [N/mm^2]$, $\gamma_{3mz} = 1.82 \times 10^{-2} [N/mm^3]$, $\eta_s = 0.5$. The spring constants in the x- and y-direction are set as $\bar{\gamma}_{mx} = \bar{\gamma}_{my} = 0.18 [N/mm]$. The material loss factor η_s took the same value as in the z-direction. The reference point for analysis is just outside the center point of the diaphragm. The vibration excitation is evenly distributed around the electrical conductor. In the experiment, the excitation is input at 300 [mV], 400 [mV], and 500 [mV], and in the analysis, the excitation force was taken to be equal to the value of the displacement measured at 100 [Hz]. Figure 5 shows an example of a nonlinear resonance using the harmonic balance method and a measured response. The horizontal axis is the excitation frequency ω . Both analytical results and measured values, which occur super harmonic resonance of order three and principal harmonic resonance. As illustrated in this figure, the calculated displacement of the diaphragm cone agrees well with the experimental data.

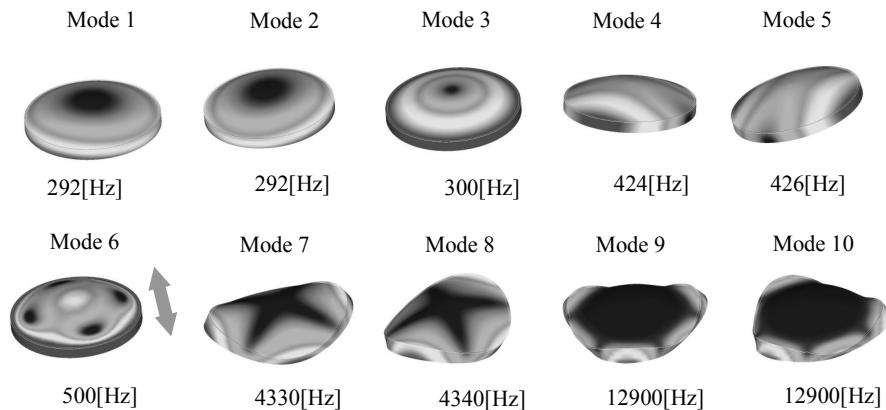


Fig. 4 Vibration modes of eigenvalue analysis

4.3 Time response and frequency analysis

By applying Runge-Kutta-Gill to Eq. (13), nonlinear time responses are calculated. We can also compare these to the diaphragm response measured by the laser displacement meter. Figs. 6(a), (b) show the frequency spectrum $A(\omega_{sp})$ of analytical and experimental results for an excitation frequency of 500 [Hz], respectively. The horizontal axis is the analysis frequency ω_{sp} . Components of the spectrum appeared at a frequency of 500 [Hz] due to the input signal and its harmonic components. Fig. 6 shows that they are in good qualitative agreement.

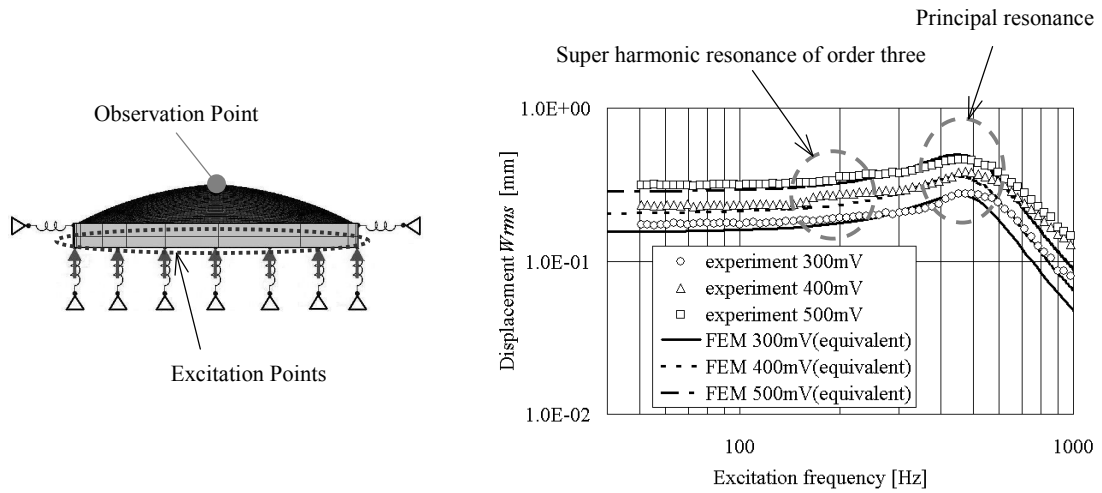


Fig. 5 Nonlinear frequency responses

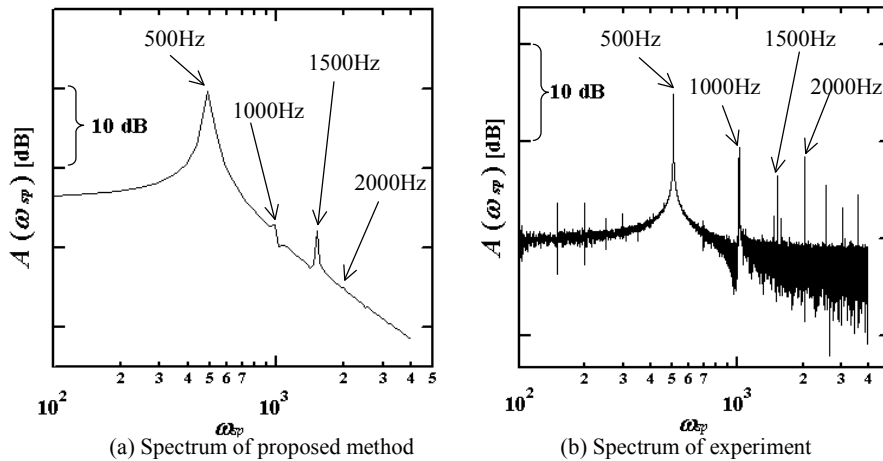


Fig. 6 Fourier spectrum of the time histories (500 [Hz])

5. Numerical simulation cases

The input would be equivalent to the F at inputting 500 [mV] in the experiment. The nonlinear resonant response is analyzed in case of the F grow up to two to four times. Further, to help understand the effects of nonlinearity, the resonant response calculates using a linear analysis program. Fig. 7 shows the results. Resonance near 500 [Hz](Mode 6) in both analyses results in almost no deformation of the diaphragm, but instead the main deformation is concentrated in the spring. In the case of linear analysis, super harmonic resonance does not appear. In the nonlinear analysis, the response has been strong hardening type nonlinearity. Focusing on the principal resonance peak, this can be seen from a shift toward higher frequencies when the displacement exceeds 0.6 [mm]. This is consistent with the trend observed in Fig. 5 of the frequency response measurement and analysis. Furthermore, a super harmonic resonance of order three appear. We can see that the nonlinearity is increased by the larger input.

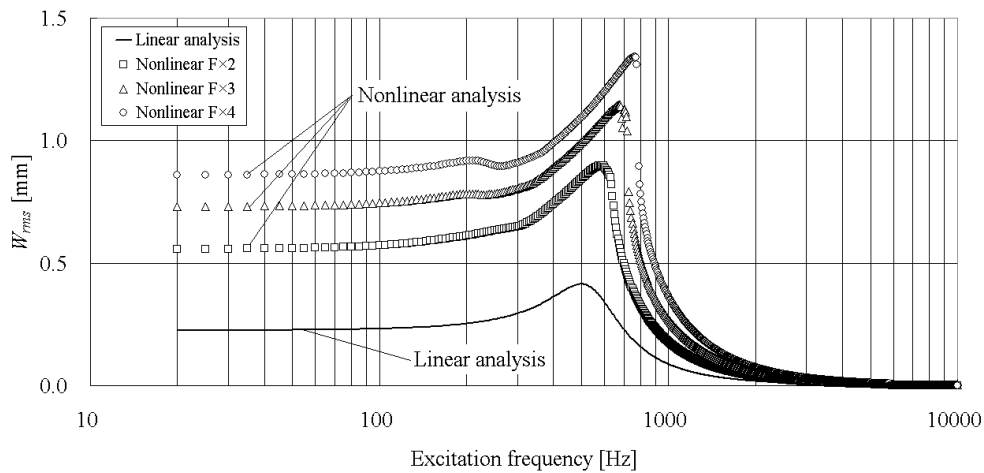


Fig. 7 Nonlinear frequency responses

6. Conclusion

We proposed a numerical method to calculate nonlinear response using FEM. To reduce dof in the computation, nodal coordinates correspond to the linear natural modes are introduced. This method was applied to the nonlinear resonant response of an elastic diaphragm for a small earphone. The diaphragm connected to multiple nonlinear springs with hysteresis. A resonant response was obtained by the proposed method. The resonant response is close to an actual response of small earphone. This confirmed that our analysis method is effective.

References

- (1) Yoshihisa, N., "Jump Phenomena in the Characteristics of Loudspeakers", Acoustical Society of Japan, Vol.14, No.2 (1958), pp.97-101.
- (2) Imaoka, K., Ohga, J., "Examination and analysis of relationship between dynamic distortion and harmonic distortion of small loudspeakers", Acoustical Society of Japan, Vol.65, No.1 (2009), pp.15-22.
- (3) Satoh, K., "Measurement of nonlinear equivalent circuit of loudspeaker", Acoustical Society of Japan, Vol.61, No.4 (2005), pp.208-218.
- (4) Satoh, K., "Measurements and Analysis of Equivalent Circuit of loudspeaker", IEICE Technical Report, EA2005-29 (2005-7), pp.25-30.
- (5) Kondo, T., Sasaki, T. and Ayabe, T., "Forced Vibration Analysis of a Straight-line Beam Structure with Nonlinear Support Elements". Transactions of the Japan Society of Mechanical Engineers, Vol.67, No.656C (2001), pp.914-921.
- (6) Pesheck, E., Boivin, N., Pierre, C. and Shaw, S. W., "Non-linear Modal Analysis of Structural Systems Using Multi-mode Invariant Manifolds", Nonlinear Dynamics, Vol.25 (2001), pp.183-205.
- (7) Yamaguchi, T., Nagai, K., Maruyama, S. and Aburada, T., "Finite Element Analysis for Coupled Vibrations of an Elastic Block Supported by a Nonlinear Spring", Transactions of the Japan Society of Mechanical Engineers, Vol. 69, No. 688C (2003), pp.3167-3174.
- (8) Yamaguchi, T., Nakahara, N., Nagai, K. Maruyama, S. and Fujii, Y., "Frequency Response Analysis of Elastic Blocks Supported by a Nonlinear Spring Using Finite Element Method", Transactions of the Japan Society of Mechanical Engineers, Vol. 70, No. 696C (2004), pp.2219-2227.
- (9) Yamaguchi, T., Saito, T., Nagai, K, Maruyama, S., Kurosawa, Y. and Matsumura, S., "Analysis of Damped Vibration for a Viscoelastic Block Supported by a Nonlinear Concentrated Spring Using FEM", Journal of System Design and Dynamics, Vol. 4, No. 1 (2011), pp.154-165.
- (10) Zienkiewicz, O.C. and Cheung, Y.K., The Finite Element Method in Structural and Continuum Mechanics (1967), MacGraw-Hill.
- (11) Wilson, E.L., Taylor, R.L., Doherty, W.P. and Ghaboussi, J., Incompatible Displacement Methods, in Numerical and Computer Methods in Structural Mechanics (1973), Academic Press.